Long-time stress relaxation in polyacrylate nematic liquid crystalline elastomers

Long-time stress relaxation in polyacrylate nematic liquid crystalline elastomers

A Hotta and E M Terentjev

Cavendish Laboratory, University of Cambridge, Madingley Road, Cambridge CB3 0HE, UK

Abstract

We study the slow relaxation of stress in polydomain acrylate liquid crystalline elastomers undergoing the alignment transition under an imposed extension. We analyse the long-time stress relaxation, the slow approach to the mechanical equilibrium and the role of time–temperature superposition. By building the master curves, we investigate extrapolated time intervals and show the presence of two distinct relaxation regimes. At the first stage, the fast power-law relaxation of stress, with the exponent 0.67, means that directional changes in nematic domains are dominant. At very long times, we find that a different, slow power law (with the exponent 0.15) becomes the dominant mode, similar to the classical results in isotropic rubbers. Model equilibrium stress–strain curves have been obtained by extrapolating the master curves. It appears that, at a true mechanical equilibrium, one finds no mesogenic effects in stress–strain, meaning that the non-trivial nematic effects could be transient, locked by network entanglements, but capable of completely relaxing by (very slow) rearrangement of network chains.

(Some figures in this article are in colour only in the electronic version)

1. Introduction

Liquid crystalline polymers (LCP) have been extensively researched by a number of groups since 1981, when the first synthesis of LCP was reported by Finkelmann *et al* [1]. The microstructure of crosslinked rubbery networks of LCP has also been widely investigated, see recent reviews [2–4]. The resulting liquid crystalline elastomers (LCE) combine remarkable properties of each of its components, liquid crystals and rubbers, but also show physical properties that place them in a separate category from any other material. Several entirely new physical phenomena have been discovered in LCE:

 (a) spontaneous, reversible shape changes of between 10–400% on temperature changes or on illumination;
 (b) the effect of 'soft elasticity'—mechanical deformation without, or with very low stress;
 (c) mechanical instabilities and discontinuous stress–strain relations on switching of nematic director by mechanical fields;

(d) electrical switching of optical properties with accompanying mechanical strains;
(e) solid phase nematohydrodynamics, with unusual rheology and anomalous dissipation and mechanical damping.

If no special precautions are taken during the LCE synthesis and crosslinking (such as, for example, [5]), the nematic polymer networks always form the polydomain director structure, essentially the Schlieren texture but with a very small characteristic size, of the order of $\xi \sim 1\,\mu$m. In a crosslinked LCE such a texture is the thermodynamic equilibrium, unlike in the ordinary 'liquid' nematics. It has been argued [6] that a quenched random disorder, introduced by network crosslinks, is responsible for the formation of polydomain structures in LCE. It has been shown that by applying external fields, in particular, uniaxial mechanical extension, the polydomain texture aligns, undergoing the 'polydomain–monodomain' (P–M) transition. The director alignment proceeds via the reorientation of correlated domains, while keeping their characteristic size ξ approximately constant, resulting in a monodomain phase where the mesogenic units are preferentially aligned along a single reference direction represented by a unit vector n [7]. During this P–M transition, the LCE sample experiences changes in its optical transparency: the amount of light scattering from remaining very narrow (localized) domain walls is small. The transition is also accompanied by a very distinct stress–strain plateau, due to the soft-elastic response of rotating nematic domains.

Research into stress relaxation in LCE, that is, rubbers with underlying orientational microstructures, has begun only recently. There are several peculiar physical effects that are not yet understood. As an example, one could mention the dependence of relaxation rate on the time the sample spends in the stretched state. Observations by several groups confirm that the director rotation in response to an applied deformation takes place faster than the equilibration of stress, so the mechanism of microstructure relaxation is not likely to be responsible for all of the phenomena. In such a situation, the key question that needs to be answered first of all is whether the true equilibrium mechanical response is ever observed experimentally, or could be reliably inferred. The answer to such a question is difficult, since very long observation times are required.

In a study of long stress relaxation after a fixed strain, Ortiz *et al* [8] have only explored intervals of time of up to several times 10^3 s, but have already shown a dramatic difference with classical rubbers and a significant role of nematic domain structure. A characteristic dual regime of long-time relaxation has been reported by Clarke and Terentjev [9], in a study where each point of stress relaxation has been examined for over 24 h. A characteristic time $t^* \sim 3000$ s separates a regime of fast power-law relaxation, $\sigma \sim t^{-0.5}$ or higher, and a very slow relaxation at later times. Experimental data have indicated that this latter regime could be described by an inverse-logarithmic law $\sigma \sim [1+\ln(t/t^*)]^{-1}$. An associated theoretical model has been able to relate the critical self-retardation to the random-disorder properties of liquid-crystalline order in the elastic network. At times before t^* the relaxation rate is dominated by an individual domain reaching its optimal condition of mechanical softness, while at later stages this approach to equilibrium is restricted by collective mechanical constraints. The model provides a relaxation rate vanishing with an essential singularity when the equilibrium is approached, due to the cooperative mechanical barriers to the rotation of each domain. The resulting kinetic equation for stress relaxation, having the form

$$\frac{\mathrm{d}}{\mathrm{d}t}\sigma = -\left(m\,\mathrm{e}^{-u/\sigma}\right)\sigma^3 \tag{1}$$

gives a solution which at short times resembles the power law $\sim t^{-1/2}$ and at longer times can be approximately interpolated as an inverse-logarithmic function, with the crossover time $t^* \approx 1/(mu^2)$.

On the other hand, since ordinary amorphous polymeric materials have their own complexities, analysing and understanding the stress relaxation has been one of the most traditional and also difficult areas in polymer physics. A large amount of work produced over many years has addressed the question of stress relaxation in rubbers; in this line, the works of Chasset, Thirion and Monnerie (cf [10]) and of Ferry [11] are most famous. By studying the natural isoprene rubber (IR) and a butadiene–styrene copolymer rubber (SBR), they were the first to mention the long-time power-law stress relaxation as well as the principles of time–temperature (t–T) superposition [12]. It has been found that the relaxation curves at a different range of elongation have their strict parallelism when they are plotted in log time–log stress having their power-law exponents always at around 0.15. A possible theoretical description has been provided in a series of papers by Curro and Pincus [13], who applied the ideas of reptation theory for a network with free dangling ends, the retraction of which has accounted for the stress relaxation law $\sigma \sim t^{-0.15}$.

In ordinary polymers, the plots of stress relaxation at constant strain versus temperature produce the same shape of curve as the plots of stress relaxation at the constant strain versus logarithm of time for the same material, which is widely known as the time–temperature superposition. The success in t–T superposition of relaxation data implies that there should be a universal relaxation law involving the temperature and time in a unique combination—the simplest example of this is the Arrhenius temperature dependence of a single relaxation time. The key contribution to this concept in polymer physics has been made by Williams, Landel and Ferry (WLF) [11, 12]. They developed a method of shifting the data horizontally along the logarithmic time scale by amounts related to temperature difference, thus obtaining a master curve of stress relaxation allowing the extrapolation of the results far beyond experimentally accessible time or temperature windows. An important concept in the WLF method is the relation between the reference temperature for t–T superposition, T_{ref}, and the glass transition point of the polymer, T_g. Various stress relaxation results can be obtained for a polymer at different temperatures. Each separate data set is obtained over a relatively few decades of time. However, by shifting each curve by a predetermined shift factor a_T, to a reference temperature T_{ref}, a master curve spanning many decades of time can be constructed. WLF derived the following empirical relationship for the shift factor a_T (see, for example, [11])

$$t \Rightarrow a_T t' \qquad \text{with} \quad \log a_T = \frac{C_1(T - T_{ref})}{C_2 + (T - T_{ref})} \tag{2}$$

where C_1 and C_2 are the empirical WLF coefficients. The values of C_1 and C_2 are often quoted in pure materials as $C_1 = -17.44$ and $C_2 = 51.6$, when the reference temperature T_{ref} is taken at the glass transition point T_g [12]. Alternatively, one finds $C_1 = -17.44$ and $C_2 = 101.6$ when T_{ref} is taken at a temperature $T_s \approx T_g + 50\,^\circ\text{C}$ [11], so it may appear that the empirical equation (2) for the shift factor is indeed universal—at least in simple polymers.

The pioneering experimental study of oscillating dynamic-mechanical properties of LCE [14, 15] has reported that for the siloxane polydomain LCE one could successfully apply the t–T superposition (treating the frequency as the inverse time) with $C_1(g) = -13.7$ and $C_2(g) = 40$, taking the reference temperature at T_g [15] (here and below, the notations $C_1(g)$ and $C_2(g)$ refer to this parametrization of the equation (2)). It should be mentioned that Gallani *et al* [14] have studied the characteristics of polydomain elastomers with nematic and smectics-A liquid crystalline phases, while Weilepp *et al* [15] have studied the behaviour of polydomain and monodomain elastomers which only have a smectics-A phase. It was found that the behaviour of the dynamic modulus does not change on going through the isotropic–nematic transition, whereas there is a marked change at the nematic–smectic-A transition.

Normally the t–T superposition cannot be successfully applied to demixed polymer blends, segregated block-copolymers, semi-crystalline and crystalline polymers. For these

more complex materials, problems are mostly encountered at temperatures near the structural transition because significant conformational changes take place at that point. This could be taken into account by using a vertical shift as well as the horizontal shift factor of the master curves. In this paper we report on the detailed study of stress relaxation after the application of constant extensional strain. Our main purpose is to investigate a different material from the siloxane LCE (a subject of [9, 14]): in a polyacrylate, photocrosslinked from a monomer state, one expects a different concentration and size of dangling ends and of crosslink clustering. We particularly focus on the issue of t–T superposition in the region of temperatures across the nematic–isotropic phase transition point T_{ni}. We have tried to adapt the WLF equation to our LCE samples, which are naturally amorphous but possess an underlying orientational symmetry breaking below T_{ni}. It is surprising to find that the WLF equation has been successful in describing the relaxation in polyacrylate LCE (certainly, the WLF concept assumes a single phase everywhere above T_g). Having built the master curve by superposing the relaxation data over a wide temperature range, we have then investigated the universal law of extrapolated stress relaxation. We find this relaxation to be extremely slow, increasingly so in the vicinity of critical stress for the P–M transition. However, in the ultimately long-time regime, after a sequence of crossovers, we have found that the 'classical' power law $\sigma \sim t^{-0.15}$ has been the dominant relaxation mode, indicating that the retraction of dangling ends is the final limiting process in a randomly crosslinked polyacrylate LCE.

This paper is organized as follows. Section 2 gives details of material preparation and experimental techniques used in this work. Section 3 describes the main results of the stress–strain measurements at different temperatures and at different rates of imposed uniaxial extension. Section 4 is dedicated to the t–T superposition of relaxation data and the construction of master curves. In section 5 we analyse the relaxation laws by fitting the master curves over very long time intervals and compare the results with some theoretical models of $\sigma(t)$ relaxation. We then conclude with a discussion of relaxation laws and the consequences of t–T superposition across the whole range of nematic and isotropic phases of LCE.

2. Experimental details

Figure 1 shows the chemical structure of the acrylate LCE used in this study, similar to the original work on this type of material performed by Legge *et al* [16]. We aimed to obtain the average crosslinking density of 10 mol% (by the reacting bonds), so that on average each chain has nine mesogenic groups between crosslinking sites: the experience of many groups tells us that in this range of crosslinking the rubber without filler particles is practically manageable in mechanical testing. Then, 0.3 mg of crosslinker and 0.03 mg of UV initiator (Irgacure 184, from CIBA) were put into 100 mg of monomers, and all the ingredients were carefully mixed. Pre-polymers were prepared on a glass plate heated up to 130 °C, well above the crystallization temperature of the monomer but low enough not to encounter chemical degradation. The samples were confined between the glass plates, which have a gap of 200 μm in order to obtain a well-defined thickness, and polymerized under the ultraviolet lamp for 60 min. The glass plates were then carefully removed to obtain free-standing rubbery films.

The issue of crosslinking uniformity is always present in the radiation-induced polymerization; due to the UV-attenuation the bottom side of a thick layer may end up with less reacting events. Gel fractions and swelling ratios of the samples were carefully measured at different stages of irradiation, to monitor the reaction rates and ensure that fully crosslinked samples would not react further, after being synthesized. The uniformity between the top and the bottom sides of the sample strip was checked by heating/cooling the free-standing films; no
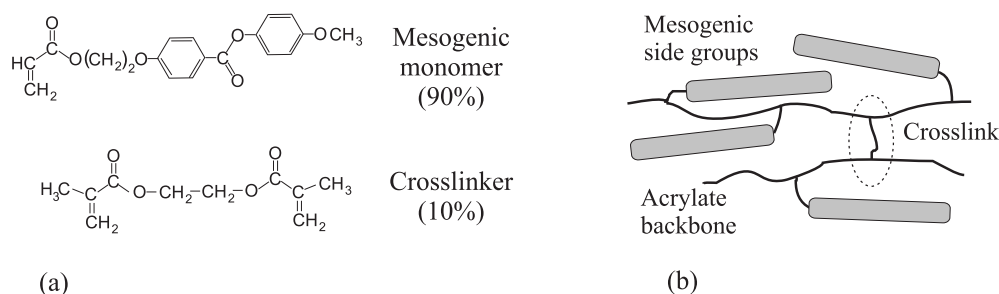
Figure 1. The polyacrylate LCE: (a) mesogenic monomers and short flexible crosslinkers before photopolymerization; (b) schematic representation of the resulting side-chain liquid crystalline elastomer.

curling, expected in a material with non-uniform elastic response, was recorded. We attribute this to the sufficiently long penetration depth of UV radiation in our materials.

Differential scanning calorimetry (DSC) measurements (Perkin–Elmer Pyris 7 DSC) were used to characterize the materials. The two phase transitions of the LCE samples were unambiguously determined to be $T_g \approx 55\,^\circ C$ and $T_{ni} \approx 90\,^\circ C$, the glass and the nematic–isotropic temperatures. No additional thermal transitions were found in the materials.

Thin uniform samples of consistent shape were prepared for the stress relaxation measurements. The samples were cut with a razor blade into a rectangular shape of approximately $10 \times 5 \times 0.2$ mm^3 (narrow elongated strips minimize the edge effects during the extensional deformation). The thickness, length and width of samples were measured by a micrometer at three points; the average of the three values was used to calculate the stress. The samples were clamped at two ends through the thermally resistant polyimide tape. The samples were extended in a step-strain fashion with the engineering strain between 0 and 1. Here, the engineering extensional strain is defined as $\varepsilon = (L - L_0)/L_0$, where L_0 is the natural unstretched length and L is the extended length of the sample imposed by the micrometer.

The force on the sample and the temperature were measured simultaneously as functions of time. For the study of long stress relaxation, a fixed step-deformation was imposed nearly instantly. In examining the stress–strain variation the strain was applied in a sequence of instant small steps, with the effective strain rate ranging from 4.6×10^{-4} s^{-1} to as low as 6.4×10^{-7} s^{-1}. These measurements were repeated for several temperatures above the glass transition.

The force values, obtained in arbitrary units, were calibrated with weights at different temperatures. Because the dynamometer sensor used here (Pioden Controls) was specially temperature compensated, only a small adjustment in the calibration with temperature was necessary. Stress values will be presented as nominal stress, σ, in units of (mN mm^{-2} $\equiv$ kPa) calculated as the measured force divided by the original cross section of the sample. The details of the custom-built stress relaxation device can be found in [17].

The natural, unstretched, length of the samples, L_0, is an important parameter—both to calculate the correct strain value and, after the end of the stretching experiment, to determine if the sample recovers its shape elastically. In each experiment, this length was determined by a separate short measurement, starting from the sample film buckled (shorter than its natural length) and gradually reaching a point when, on increasing the distance between its clamped ends in very small steps, the stress response suddenly increases indicating that the rubber is being stretched.

The samples were then extended to a certain fixed strain and kept at a constant temperature to monitor stress relaxation. The sample preparation history, including the rate of imposed
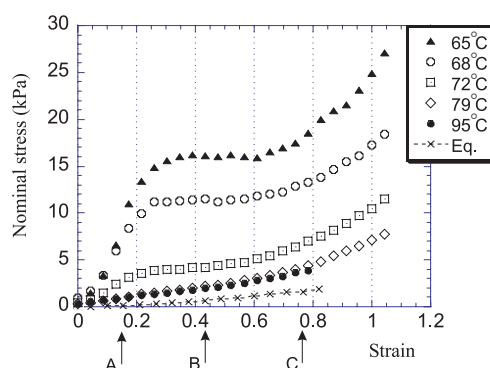
Figure 2. The stress–strain curves obtained at a fixed strain rate, 1.45×10^{-4} s^{-1}, at a sequence of different temperatures: 65 °C ($T/T_{\text{ni}} = 0.93$); 67.5 °C ($T/T_{\text{ni}} = 0.94$); 71.8 °C ($T/T_{\text{ni}} = 0.95$); 79 °C ($T/T_{\text{ni}} = 0.97$); and 94.7 °C ($T/T_{\text{ni}} = 1.01$). The decrease of the soft stress plateau and of the range of strains for the P–M transition correspond to the theoretical ideas and previous experimental work, cf [6]. The lowest curve, labelled Eq., represents the extrapolated equilibrium stress–strain values (see text for details).

strain and the total time of relaxation, was kept constant throughout the whole series of experiments.

3. Polydomain–monodomain transition in stress–strain curves

Figure 2 shows all the results of stress–strain measurements at different temperatures at a constant strain rate of 8.7×10^{-3} min^{-1} or 1.45×10^{-4} s^{-1}, in steps of $\Delta\varepsilon \approx 0.04$. The temperature of each experiment ranges from 65 to 94.7 °C (rounded figures labelled on the plot). The samples are stretched from 0 to 1 (100%) in nominal strain. Here the clear soft plateau area between the strains of 0.2–0.6 reveals the P–M transition [6], where there is no increase in stress even if we continue to impose strain on the sample.

This P–M transition has been theoretically explained by applying the concept of randomly quenched disorder introduced by network crosslinks. Fridrikh and Terentjev [6] have shown that the system possessing the property of soft elasticity can benefit from rotating the local nematic director in each domain of its disordered texture. When a threshold stress is reached, the correlated nematic domains begin to rotate, aligning towards the direction of extension. Since the average polymer backbone is prolate along the local nematic director n [16], the aligning of average n results in the effective lengthening of the whole sample, thus accommodating the imposed strain and creating the soft stress plateau over a large interval of deformations. This soft plateau, which is typical of the P–M transition [18], can be seen nearly up to 94 °C, where the sample reaches its clearing point T_{ni} in our experiments. The curve which is named 'equilibrium' in figure 2 is the calculated set of data obtained by extrapolation of the relaxation master curves (see below). The detailed analysis of relaxation laws will follow; here we would like to emphasize that seemingly there is no stress plateau in the 'equilibrium' curve.

Figure 3 shows the results of the stress–strain measurements at different continuous strain rates at a constant temperature 69.8 °C ($T/T_{\text{ni}} = 0.94$). The strain rates were controlled from 6.4×10^{-7} to 4.6×10^{-4} s^{-1} by way of imposing a small instant strain step and waiting for a certain fixed time before the next step—the time between steps is labelled on the plot. The overall strain has been increasing from 0 to 1.1 (110%). Here also, the clear soft plateau
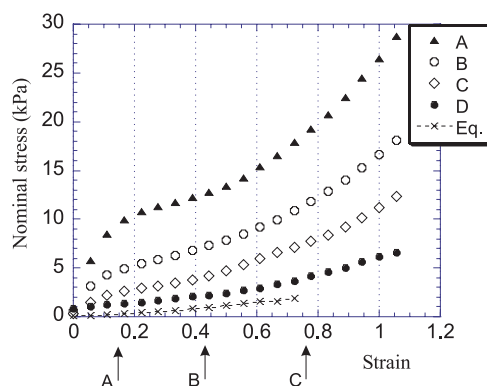
Figure 3. Stress–strain curves at a fixed temperature well below the nematic transition, $T/T_{ni} = 0.94$, and at different strain rates: A, 4.6×10^{-4} s^{-1}; B, 1.9×10^{-4} s^{-1}; C, 3.7×10^{-5} s^{-1}; D, 6.4×10^{-7} s^{-1} (one full day of relaxation between each strain point). The lowest curve, Eq., is the same as in figure 2.
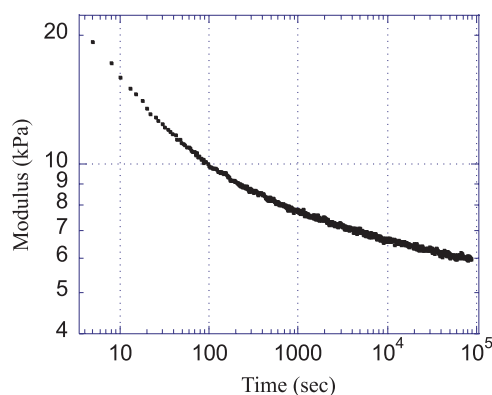
Figure 4. An example of a stress relaxation curve at a fixed temperature (82.5 °C, $T/T_{ni} = 0.98$) and strain ($\varepsilon = 0.222$). It is evident that a substantial relaxation of internal stress occurs in the material and that an equilibrium is far from being reached. An efficient extrapolation technique is needed to predict the final equilibrium value of stress.

reveals the P–M transition. As in figure 2, this plateau can be seen up to the lowest strain rate of 6.4×10^{-7} s^{-1}. The lowest 'equilibrium' curve here is the data extrapolated in the same way as in figure 2.

In the next section we show that the time–temperature superposition is applicable in this polyacrylate LCE material. This implies that these two 'equilibrium' curves, in figures 2 and 3, are exactly the same curve. This would be the truly equilibrium stress–strain variation if we waited for the stretched sample to be completely relaxed after each step increment, or equally, if we made the measurement at such a high temperature that all relaxation processes would be completed at a given strain rate. This leads to a paradoxical conclusion that the equilibrium mechanical response of a nematic LCE, undergoing a P–M transition, is not different from that of a high-temperature isotropic elastomer. We discuss this point, and its consequences, at much greater length towards the end of this paper.
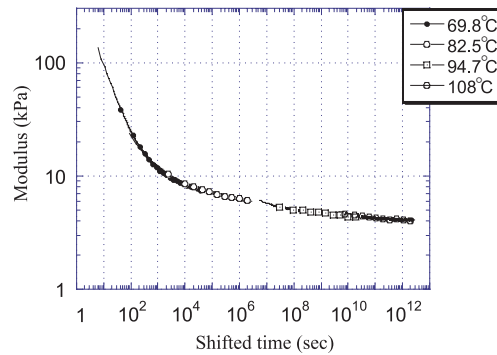
Figure 5. An example of a master curve obtained by t–T superposition of relaxation data at different temperatures, corresponding to the selected constant value of imposed strain $\varepsilon = 0.222$. Note that the last two portions of the master curve are obtained at temperatures above T_{ni}, yet the overall superposition seems to be successful.
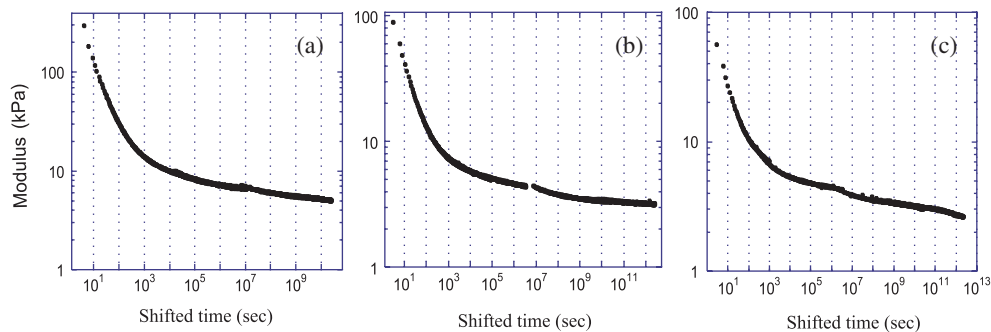

Figure 6. A collection of three master curves, the results of t–T superposition for different constant values of strain labelled in figure 2: A, $\varepsilon = 0.166$; B, $\varepsilon = 0.444$; C, $\varepsilon = 0.778$.

4. Time–temperature superposition

Stress relaxation curves were measured at several different temperatures. One example of such a relaxation curve can be seen in figure 4. We plot the effective extension modulus, $E(t)$, the coefficient of a nominal linear relation $\sigma(t) = E(t)\varepsilon$ in response to a constant strain ε applied at $t = 0$. This particular curve was taken at 82.5 °C ($T/T_{ni} = 0.98$) at the strain of 0.222, for a period of 24 h.

Figure 5 shows one of the results of time–temperature superposition of several stress–strain curves measured at 69.8 °C ($T/T_{ni} = 0.94$), 82.5 °C ($T/T_{ni} = 0.98$), both below T_{ni}, then 94.7 °C ($T/T_{ni} = 1.01$), nearly at T/T_{ni}, and 108 °C ($T/T_{ni} = 1.05$), well above T/T_{ni}, all at the constant value of 0.222 in the applied strain.

Stress relaxation curves measured at the different constant values of strain have been superimposed in order to gain the corresponding master curves by way of shifting each relaxation curve above 69.8 °C, using the same shift factors as in figure 5. The reference temperature was taken at 69.8 °C which is 14.8 °C above the T_g of the sample. Figure 6 shows three more of the typical superimposed master curves which have been taken from these stress–strain experiments at $\varepsilon = 0.166$ (point A, labelled by an arrow in figure 2), $\varepsilon = 0.444$ (point B) and $\varepsilon = 0.778$ (point C). These three strain points are at different positions with respect to
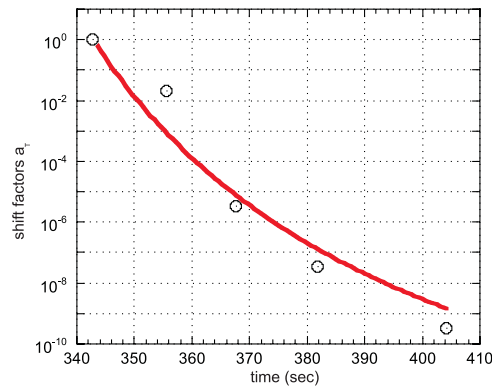
Figure 7. Shift factors at different temperatures fitted with the WLF equation (2). The WLF coefficients are $C_1 = -17.44$ and $C_2 = 60.0$, which are similar to the values obtained for normal crosslinked rubbers.

the P–M transition, before the threshold, on the stress plateau and in the aligned state past the transition. It is surprising that all four curves (including that in figure 5 at $\varepsilon = 0.222$), which were obtained from different physical states, can be superimposed in the same way using all the same shift factors a_T. Remarkably, the time–temperature superposition is applicable through all the strains we measured, regardless of its phase, that is, the polydomain, the monodomain or the mixed transient phase.

To illustrate this universality, the shift factors used to construct all master curves (at all strains) are then plotted in a classical WLF graph, figure 7. Through the whole range of strains (before, during and after the P–M transition) we were able to keep a constant shift factor for each temperature. Fitting the curves with the WLF equation is successful, giving the coefficients $C_1 = -17.44$ and $C_2 = 60.0$, which are very close to the classical results of Ferry *et al*.

All these results indicate that the t–T superposition is effective in our liquid crystalline elastomer and can be done similarly to ordinary vulcanized rubbers. This means that the liquid crystalline elastomer, in true mechanical equilibrium, would perform exactly the same as normal rubbers.

5. Fitting the master curves

All master curves having been made by t–T superposition were fitted with several stress relaxation equations. A number of theoretical models have been applied to fit the stress relaxation curves. Among those equations, the power law and the logarithmic law seem to be effective for our samples. The fitting equations we used in this analysis are

Fast power law $\qquad \sigma = m_1 + m_2 t^{-0.67}$ $\qquad\qquad\qquad\qquad\qquad\qquad$ (3)

Slow power law $\qquad \sigma = m_1 + m_2 t^{-0.15}$ $\qquad\qquad\qquad\qquad\qquad\qquad$ (4)

Logarithmic law $\qquad \sigma = m_1 + m_2/[1 + \log(t/t^*)]$ $\qquad$ with $\quad t^* \approx 1000$ s. $\qquad$ (5)

In each case, only two fitting parameters were used after the crossover time and the power exponent have been identified, confirmed to remain the same at all strains and then used as a known value.

Figure 8 shows the fitting results at a strain of 0.222. It seems that at long relaxation after t^* both the power law, having its power exponent $\sim$0.15, and the logarithmic law are
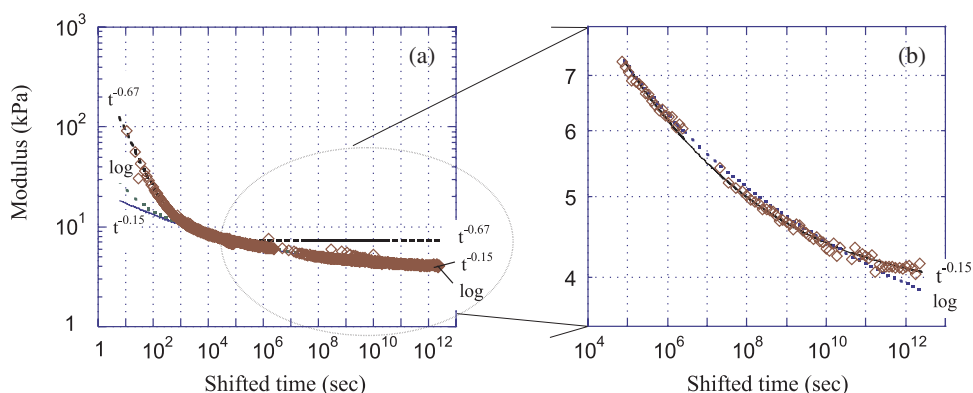
Figure 8. Fitting of stress relaxation master curve. (a) Power law $t^{-0.67}$ matches very well with the experimental data at the first stage, approximately up to $t^* \sim 1000$ s. (b) Power law $t^{-0.15}$ is effective at times after the crossover t^*. Although the logarithmic law also seems to be applicable, it starts deviating after $\sim 10^{10}$ s as shown by the dotted curve in (b).

reasonably good fits. However, if we magnify the graph, we can easily see the deviation in the logarithmic fitting at longer relaxation time especially at lower strain where the sample is in a linear stress–strain regime.

Thus, we conclude that our polyacrylate LCE rubbers initially relax, obeying the power law with the exponent of ≈ 0.67 (it may be a pure coincidence that this is indistinguishable from $\frac{2}{3}$). This is consistent with earlier observations of initial fast power-law relaxation [8, 9], although the exponent is higher in our polyacrylate LCE. At a much later stage, after the crossover at $t^* \sim 1000$ s, the stress relaxation becomes much slower—which is again consistent with reports in the literature. The long-time relaxation follows the power law with the exponent of around 0.15. The logarithmic law could only be applied to the data in the very broad crossover region; at shifted times corresponding to 10^{10} s the deviation between it and the power law of 0.15, better fitting the data, is evident.

In other words, at late stages of relaxation, the LCE behaves similarly to a normal isotropic network, relaxing with the power law $\sigma \sim t^{-0.15}$—presumably due to the same Curro–Pincus mechanism of dangling end retraction. In this regime we can no longer see the mesogenic effect. This means that the nematic degrees of freedom finish their evolution after $t \sim t^*$ and the overall relaxation behaviour reverts to the way the ordinary vulcanized rubbers relax. This is the reason why the t–T superposition works in our samples through the whole range of temperatures over the nematic–isotropic temperature T_{ni}. Above T_{ni} one finds an ordinary isotropic rubbery phase where the material has to behave as ordinary rubber, relaxing with the power law having its exponent at around 0.15. Below T_{ni} and at times earlier than the crossover t^*, the fast power-law stress relaxation is clearly dominated by the nematic domain orientational effects.

6. Conclusion

Now that we know that the t–T superposition works and the master curve fittings have been performed, we can predict the value of the stress at infinite relaxation time. Carrying out the data fittings through all the strain points, we obtain the extrapolated 'equilibrium' stress–strain curves which can never be reached in real experimental time. These curves are shown in figures 2 and 3 and, indeed, the two 'equilibrium' curves extrapolated in time, or in temperature,
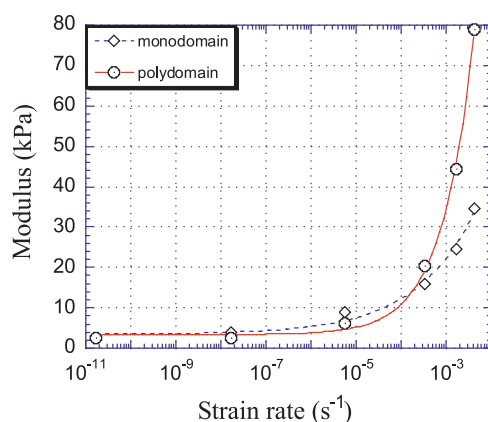
Figure 9. Effective extension moduli obtained in monodomain and polydomain states of LCE, by taking a slope of a corresponding stress–strain curve at different strain rates. The polydomain modulus increases more dramatically with raising the strain rate, implying that the 'non-equilibrium' nematic effect is stronger in a polydomain state. However, if we wait for a very long time, both extrapolated moduli converge to the same value of 2.50 kPa.

are exactly the same. These extrapolated 'equilibrium' results indicate that the stress–strain curve does not seem to have a soft plateau region. That is, if we wait infinitely for the sample to relax completely at each point of the stress–strain experiment we cannot see the typical mechanical response seen in LCE samples undergoing the P–M transition. This could mean that if we wait for a long time, enough for the nematic director orientation to relax, the mode of relaxation can be shifted from the mesogenic stress relaxation mode to ordinary rubber relaxation mode.

As a possible reasoning for the present findings, we could venture a suggestion that the macroscopic coupling between the nematic director and the average backbone anisotropy of a polymer network (as opposed to the microscopic coupling due to the side-group spacer) is not inherent and is only a transient condition, locked by dense network entanglements. Little is known theoretically about the dynamics of entangled and permanently crosslinked networks, even in the isotropic state and in equilibrium; the recent tube model calculation of nematic rubber elasticity [19] refers to only a few similar equilibrium theories for classical entangled rubber. In the dynamical response, the difficulties of interpreting, for instance, the constraint release by retraction of loops and the interplay between stress alignment and the nematic alignment explain the absence of any adequate theory. The overall experimental picture acquired over the years of study of nematic elastomers indicates that, at relatively short times of mechanical testing (which are the only experimentally accessible times, in practice), the overall network shape and the local nematic director are linked together. However, it now appears that, if a sufficient time is given to the network strands, at each stage of deformation they could find a true equilibrium shape after disentanglement. In this state, the conformation of backbones and their response to deformation seem to be indistinguishable from that of a classical isotropic rubber.

Another illustration of this is given in figure 9, which shows the effective moduli, obtained as the gradients of the stress–strain curve in both polydomain and monodomain areas (avoiding the soft plateau region as a clearly transient state), from the plot in figure 3 at 69.8 °C. The polydomain moduli are estimated by taking the slope before the soft plateau, for strains ranging from 0 to 0.2. The effective monodomain modulus is obtained as a slope at $\varepsilon > 0.8$. One can

see a strong dependence on the effective strain rate (the lines are a guide to the eye) and the final 'equilibrium' value approached at $\dot{\varepsilon} \to 0$ from the extrapolated master curves. Consistently with the above discussion, this extrapolated value is the same, approximately 2.50 kPa. This is the only 'equilibrium' rubber modulus of our acrylate LCE (at 69.8 °C) regardless of which phase, such as polydomain or monodomain phases, the samples are in. Consistently with the previous studies of nematic rubber elasticity, at faster strain rates (or shorter relaxation times) the moduli are very different. The polydomain modulus has a stronger dependence on strain rate, meaning that nematic effects in the mechanical response are more significant here than in a monodomain state stretched along the director.

The features of mechanical response of acrylate LCE have been discussed. Non-equilibrium stress–strain measurements have been performed and every effort has been taken to detect the final equilibrium mechanical properties. The main conclusion of this paper is the applicability of t–T superposition and the universality of its WLF coefficients. Fitting the master curves reveals that the longest relaxation mode in our acrylate LCE is the slow power law $\sigma \sim t^{0.15}$, well known in classical rubbers. It appears that the question of coupling between nematic and rubber degrees of freedom is less clear than it was previously thought and much more work is needed to understand which LCE states and which effects are transient, albeit extremely long-lived, and which are the true equilibrium.

Acknowledgments

References

[1] Finkelmann H, Koch H J and Rehage G 1981 *Macromol. Rapid Commun.* **2** 317
[2] Warner M and Terentjev E M 1996 *Prog. Polym. Sci.* **21** 853
[3] Brand H R and Finkelmann H 1998 *Handbook of Liquid Crystals* vol 3, ed D Demus *et al* (New York: Wiley) ch 5
[4] Terentjev E M 1999 *J. Phys.: Condens. Matter* **11** 239
[5] Küpfer J and Finkelmann H 1991 *Macromol. Rapid Commun.* **12** 717
[6] Fridrikh S V and Terentjev E M 1999 *Phys. Rev.* E **60** 1847
[7] Clarke S M, Terentjev E M, Kundler I and Finkelmann H 1998 *Macromolecules* **31** 4862
[8] Ortiz C, Ober C K and Kramer E J 1998 *Polymer* **39** 3713
[9] Clarke S M and Terentjev E M 1998 *Phys. Rev. Lett.* **81** 4436
[10] Chasset R and Thirion P 1965 *Proc. Conf. on Physics of Non-Crystalline Solids* ed J A Prins (Amsterdam: North-Holland) p 345
[11] Ferry J D *Viscoelastic Properties of Polymers* (New York: Wiley)
[12] Williams M L, Landel R F and Ferry J D 1955 *J. Am. Chem. Soc.* **77** 3701
[13] Curro J G and Pincus P 1983 *Macromolecules* **16** 559
[14] Gallani J L, Hilliou L, Martinoty P, Doublet F and Mauzac M 1996 *J. Physique* II **6** 443
[15] Weilepp J, Zanna J J, Assfalg N, Stein P, Hilliou L, Mauzac M, Finkelmann H, Brand H R and Martinoty P 1999 *Macromolecules* **32** 4566
[16] Legge C H, Davis F J and Mitchell G R 1991 *J. Physique* II **1** 1253
[17] Clarke S M and Terentjev E M 1999 *Faraday Discuss.* **112** 325
[18] Uchida N 2000 *Phys. Rev.* E **62** 5119
[19] Kutter S and Terentjev E M 2001 *Eur. Phys. J.* E **21** at press
(Kutter S and Terentjev E M 2001 *Preprint* cond-mat/0106193)